Feng Huang, Tyrone O. Rooney, Ji-Feng Xu, and Yun-Chuan Zeng, 2020, Magmatic record of continuous Neo-Tethyan subduction after initial India-Asia collision in the central part of southern Tibet: GSA Bulletin, https://doi.org/10.1130/B35444.1.

Supplemental Material

1 Analytical Methods

1.1. Zircon U-Pb dating and Hf isotope analyses

1.2. Whole-rock major, trace elemental and Sr-Nd isotopic geochemical analyses

1.3. Geochemical modeling by Arc Basalt Simulator version 5 (ABS5)

2. Analytical data and modeling results

Table S1. SIMS U-Pb zircon dating results for Dazi mafic rocks

Table S2. LA-ICP-MS U-Pb zircon dating results for Dazi mafic samples

Table S3. Hf isotopic results of Dazi mafic rocks

Table S4. Major, trace element and Sr-Nd isotopic data of Dazi mafic samples

Table S5. Calculation results of PRIMACALC2 for primary magma compositions of representative mafic samples from Dazi area, southern Tibet

Table S6. Forward modeling results of ABS5

3. REFERENCES CITED

1. ANALYTICAL METHODS

1.1. Zircon U-Pb dating and Hf isotope analyses

Zircon has become the most widely useful minerals for the extraction of information on the prehistory and genesis of magmatic rocks. We chose ten fresh mafic samples from Dazi County. Zircon concentrates were separated from ~20 kg of each sample using standard density and magnetic separation techniques, however, the amount of zircon grains were less than 200. Zircon grains, together with zircon standard 91500, TEMORA and Qinghu, were set in epoxy mounts, which were then polished to expose the interior of the grains. They were then imaged by CL using a Carl Zeiss SUPRA55SAPPHIR field emission-scanning electron microscope connected to a Gatan Mono CL4 system at Guangzhou Institute of Geochemistry, Chinese Academy of Sciences (GIGCAS), Guangzhou, China. Transmitted, reflected light and CL images were used to check the internal structures of individual zircon grains and to select potential target sites for U-Pb dating and Hf isotope analyses. Secondary ion mass spectrometry (SIMS) zircon U-Pb analyses for four mafic samples (10LKE-01, 11DZ-20, 13DZ-09 and 13DZ-11) were conducted using a CAMECA IMS1280-HR system at GIGCAS. Analytical procedure is similar to that described by Li et al. (2009). The O_2^- primary ion beam with an intensity of ~10 nA was accelerated at −13 kV. The analyzed spot is ~20 μm × 30 μm in size. The aperture illumination mode (Kohler illumination) was used with a 200 μm primary beam mass filter (PBMF) aperture to produce even sputtering over the entire analyzed area. Oxygen flooding was used to increase the O^2 pressure to 5×10^{-6} Torr in the sample chamber, enhancing Pb^+ sensitivity to a value of ~25 cps/nA/ppm for zircon. This great enhancement of Pb^+ sensitivity is crucial to improve precision of $^{207}Pb/^{206}Pb$ zircon measurement. Positive secondary ions were extracted with a 10 kV potential. In the secondary ion beam optics, a 60 eV energy window was used, together with a mass resolution of ~5400. Rectangular lenses were activated in the secondary ion optics to increase the transmission at high mass resolution. A single electron multiplier was used in ion-counting mode to measure secondary ion beam intensities by the peak jumping sequence: 196 ($^{90}Zr_2{}^{16}O$, matrix reference), 200 ($^{92}Zr_2{}^{16}O$), 200.5 (background), 203.81 ($^{94}Zr_2{}^{16}O$, for mass calibration), 203.97 (Pb), 206 (Pb), 207 (Pb), 208 (Pb), 209 ($^{177}Hf^{16}O_2$), 238 (U), 248 ($^{232}Th^{16}O$), 270 ($^{238}U^{16}O_2$), and 270.1 (reference mass). The integration time for these masses are 1.04, 0.56, 4.16, 0.56, 6.24, 4.16, 6.24, 2.08, 1.04, 2.08, 2.08, 2.08, and 0.24 s, respectively. Each measurement consisted of seven cycles, and the total analytical time per measurement was ~12 min. Calibration of Pb/U ratios is relative to the standard zircon Plesovice (337 Ma; Sláma et al., 2008), which was analyzed once every four unknowns, based on an observed linear relationship between *ln* ($^{206}Pb/^{238}U$) and *ln* ($^{238}U^{16}O_2/^{238}U$) (Whitehouse et al., 1997). A long-term uncertainty of 1.5% (1 RSD) for $^{206}Pb/^{238}U$ measurements of the standard zircons was propagated to the unknowns, despite that the measured $^{206}Pb/^{238}U$ error in a specific session is generally around 1% (1 RSD) or less. U and Th concentrations of unknowns were also calibrated relative to the standard zircon Plesovice, with Th and U concentrations of 78 and 755 ppm, respectively (Sláma et al., 2008). Measured compositions were corrected for common Pb using non-radiogenic ^{204}Pb. The fraction of common Pb is very low, and is largely derived from laboratory contamination introduced during sample preparation (Ireland and Williams, 2003). An average of present-day crustal composition (Stacey and Kramers, 1975) is used for the common Pb. A secondary standard zircon Qinghu (Li et al., 2013) were analyzed as unknown to monitor the reliability of the whole procedure. Eleven analytical spots conducted during the course of this

study yield a concordia age of 158.8 ± 1.7 Ma, identical to its recommended value (159.5 ± 0.2 Ma; Li et al., 2013). Uncertainties on single analyses are reported at the 1σ level; mean ages for pooled U-Pb analyses are quoted with a 95% confidence interval. Data reduction was carried out using the Isoplot/Ex 3 software (Ludwing, 2003). To evaluate the reliability of the dating results of the mafic dykes, six other mafic samples (11DZ-06, 11DZ-10, 11DZ-21, 11DZ-23, 13DZ-10, 13DZ-15) were analyzed by the laser ablation inductively coupled plasma mass spectrometry (LA-ICPMS) at GIGCAS. Together, U-Pb dating and trace element analyses of these six samples were performed synchronously by LA-ICP-MS. Every ten sample analyses were followed by two analyses of NIST SRM 610 glass to correct the time-dependent drift of sensitivity and mass discrimination for the trace element analysis. Laser ablation equipped a pulsed Resonetics RESOlution 193 nm ArF excimer laser, conducted at a constant energy of 80 mJ, with laser pulse frequency of 6 Hz and a spot diameter of 30 μm. An Agilent 7500a ICP-MS instrument was used to acquire ion-signal intensities. Helium was used as a carrier gas. Argon was used as the make-up gas and mixed with the carrier gas via a T-connector before entering the ICP. Details of instrumental conditions and data acquisition refer to Huang et al. (2017). NIST SRM 610 glass (Gao et al., 2002) and TEMORA zircon standards ($^{206}Pb/^{238}U$ age = 416.8 ± 1.1 Ma, Black et al., 2003) are used as external standards. A second zircon standard GJ-1 was analyzed as unknown samples and 19 grains yielded a mean age of 608.2 ± 2.3 Ma, which is consistent with previous studies (608.5 ± 0.4, Jackson et al., 2004). This result suggests instrument for zircon U-Pb dating was working properly. Off-line inspection and integration of background and analyte signals, and time-drift correction and quantitative calibration for trace element analyses and U-Pb dating were performed using ICPMSDataCal software (Liu et al., 2008). Concordia diagrams and weighted mean calculations were made by using Isoplot/Ex 3 program (Ludwing, 2003). Zircon Hf isotopic analyses were conducted on the dated zircons using a Neptune Plus MC–ICP-MS in combination with a Resonetics RESOlution 193 excimer ArF laser ablation system, at GIGCAS. Analytical spots were located close to or on the same domain of LA–ICP-MS spots. The analyses were conducted with a beam diameter of 45 μm. Normally, a signal intensity of >5 V at ^{180}Hf mass can be obtained using the laser repetition rate of 8 Hz with energy of 80 mJ. The ablated material was transported in a helium carrier gas with addition of a small flow of nitrogen. Data acquisition for each analysis consists of 30 s gas background collection and 30 s signal collection for laser ablation. A signal collection model for one block includes 200 cycles, in which one cycle has 0.131 s integration time. Every 6 sample analyses were followed by two analysis of Penglai and GJ-1zircon standards. The measured isotopic ratios of $^{176}Hf/^{177}Hf$ were normalized to $^{179}Hf/^{177}Hf = 0.7325$, using exponential correction for mass bias. In order to obtain accurate $^{176}Hf/^{177}Hf$ ratios, the isobaric interferences of ^{176}Lu and ^{176}Yb on ^{176}Hf must be corrected. The ratios of $^{176}Lu/^{175}Lu = 0.02655$ and $^{176}Yb/^{171}Yb = 0.90184$ obtained during Hf analysis on the same spot were used in the isobaric interference correction (Wu et al., 2006). The details for data calibration could be found in Huang et al. (2017). Replicate analysis of Penglai zircon standard give a mean $^{176}Hf/^{177}Hf$ ratio of 0.282898 ± 0.000010 (2σ, n = 44), which is consist with previous studies (0.282906 ± 0.000010; Li et al., 2010). Replicate analysis of GJ-1 zircon standard give a mean $^{176}Hf/^{177}Hf$ ratio of 0.282007 ± 0.000005 (2σ, n = 44), which is consistent with previous studies (0.282000 ± 0.000005, Morel et al., 2008; 0.282013 ± 0.000003, Yuan et al., 2008). The decay constant for ^{176}Lu is 1.867×10^{-11}/year (Söderlund et al., 2004) and the chondritic ratios of $^{176}Hf/^{177}Hf$ and $^{176}Lu/^{177}Hf$ used in calculations are 0.282772 and 0.0332 (Blichert-Toft and Albarede, 1997), respectively. Initial zircon $^{176}Hf/^{177}Hf$ ratios and $\varepsilon_{Hf}(t)$ values are calculated based on the zircon $^{206}Pb/^{238}U$ ages.

1.2. Whole-rock major, trace elemental and Sr-Nd isotopic geochemical analyses

Selected fresh whole-rock samples were crushed and ground in an agate ring mill, and the final powder was used for analyses of major and trace elements as well as Sr–Nd isotopes. Major elements were determined using a Rigaku ZSX100e X-ray fluorescence (XRF) spectrometry, whereas trace element contents were measured with a Thermo iCAP Q inductively coupled–plasma mass spectrometer (ICP-MS) at GIGCAS. The analytical procedures followed those described by Huang et al. (2015). Analytical uncertainties are ± 5% for major elements. The uncertainties in the analyses of internal standards and trace elements are ± 5% for REEs and ± 5%–10% for trace elements. The methods used for the chemical separation of Sr and Nd were similar to those described by Huang et al. (2017). Sr isotopic compositions of the mafic samples were measured using a static multiple Faraday collector with a thermal ionization mass spectrometer (TIMS, Thermo-Finnigan TRITON). The Nd isotopic compositions were measured using a Micromass Isoprobe multi-collector-inductively coupled plasma-mass spectrometer (MC-ICP-MS). All measured $^{143}Nd/^{144}Nd$ and $^{86}Sr/^{88}Sr$ ratios were fractionation corrected to $^{146}Nd/^{144}Nd = 0.7129$ and $^{86}Sr/^{88}Sr = 0.1194$, respectively. The $^{87}Sr/^{86}Sr$ value of the NBS 987 standard and the $^{143}Nd/^{144}Nd$ ratio of the JNdi-1 standard were 0.710256 ± 6 (2σ) and 0.512108 ± 11 (2σ), respectively, which are consist with previous studies (NBS 987 $^{87}Sr/^{86}Sr = 0.710251 \pm 0.000013$; Balcaen et al., 2005; JNdi-1 $^{143}Nd/^{144}Nd = 0.512112 \pm 0.000028$; Chu et al., 2009). The decay constant for ^{87}Rb and ^{147}Sm are 1.42×10^{-11}/year (Steiger and Jager, 1977) and 6.54×10^{-12}/year (Lugmair and Marti, 1978). The chondritic ratios of $^{143}Nd/^{144}Nd$ and $^{147}Sm/^{144}Nd$ used in calculations are 0.512638 and 0.1967 (Jacobsen and Wasserburg, 1980), respectively. Initial whole rock $^{87}Sr/^{86}Sr$ and $^{143}Nd/^{144}Nd$ ratios are calculated based on the weighted mean $^{206}Pb/^{238}U$ ages.

1.3. Geochemical modeling by Arc Basalt Simulator version 5 (ABS5)

The detailed operation tutorial could be found in Kimura (2017). Here we simply describe the modeling process. There are different worksheets in the ABS5 Excel workbook, but most of them are used for calculations and should not be changed. Only yellow cells with red characters in the [CONTROL PANEL] and [DATA INPUT] worksheets should be changed. First, we choose the appropriate parameters and input them in the [CONTROL PANEL] sheet (Figure S1). At the top left, we choose PM (primitive mantle) as the denominator composition in multi-element plots. Then we use the primary magma composition of 11DZ-06 and 11DZ-19 to model, the primary magma compositions could be found in the [DATA INPUT] worksheet. Because the amphibole is the phenocryst phase in the mafic samples, we prefer the SLAB SOLIDUS MODEL as Wet solidus. We also choose W (Workman and Hart, 2005) as model peridotite compositions (PERID) for Neo-Tethyan subduction. As discussed in the text, the southern Tibet is an Andean-type subduction environment, thus we choose the North Chile and Colombia-Ecuador subduction zones as the SLAB P–T MODEL condition.

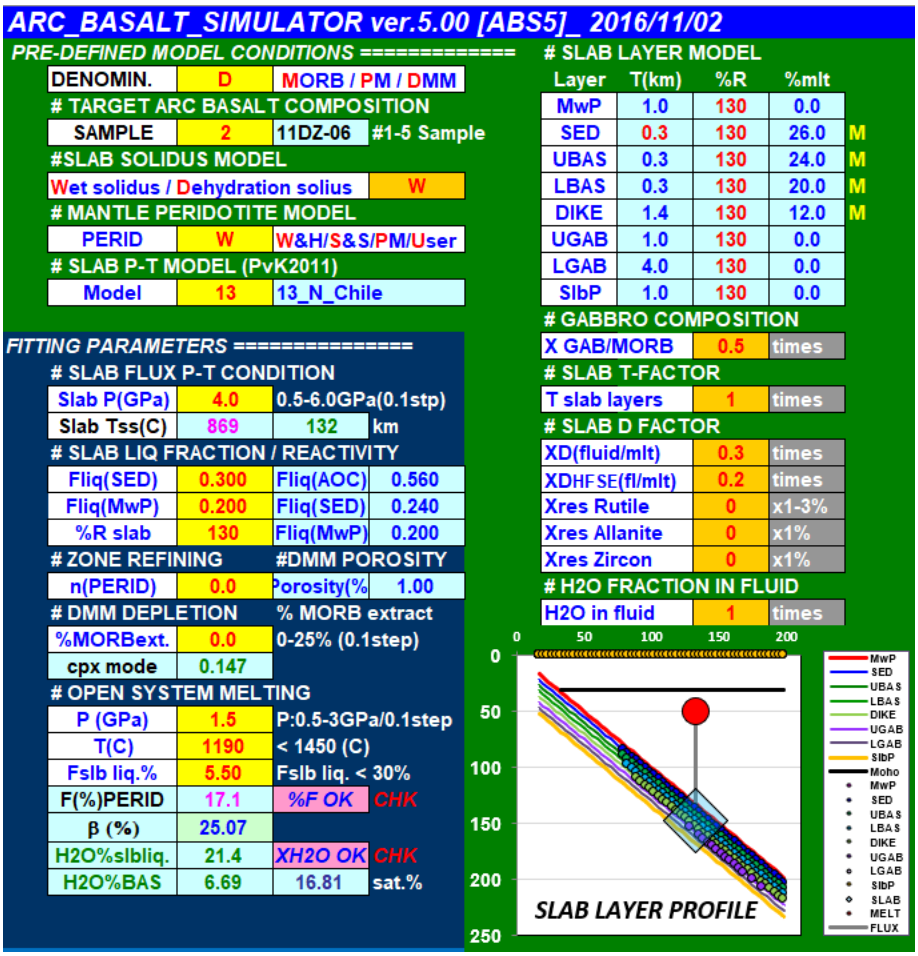

Fiugure S1 Pre-defined conditions in ABS5 shown in the [CONTROL_PANEL] (Kimura, 2017).

To generate a model appropriate for samples, we use the PRIMACALC2 (Kimura and Ariskin, 2014) to calculate the primitive magma compositions. The results show NiO in the olivine within the primary magma satisfies the mantle-olivine Ni-Fo array of mantle equilibrium. Then we input primitive magma compositions of samples 11DZ-06 and 11DZ-19 calculated by into the [DATA INPUT] worksheet (Figure S2). The trace element compositions of the source materials are assumed from the geochemistry of the subducting materials (Kimura and Ariskin, 2014). We choose the updated GLOSS II as the ocean sediment for SED (Plank, 2014), the other parameters all refer to Kimura (2017).

Target basalt compositions
[Input target basalt values]

	1	2	3	4	5
Element/SP	11DZ-19	11DZ-06			
SiO2	51.33	52.86			
TiO2	0.70	0.69			
Al2O3	13.71	13.24			
Fe2O3	10.04	8.87			
MgO	13.44	13.40			
CaO	8.76	8.08			
Na2O	2.32	2.26			
K2O	0.48	1.31			
SUM	100.78	100.70			
Rb	8.317	44.534			
Ba	99.874	171.644			
Th	1.165	4.130			
U	0.400	1.322			
Nb	1.578	2.641			
Ta	0.111	0.267			
K	3804.879	10439.95			
La	5.577	8.770			
Ce	12.521	19.006			
Pb	4.538	4.676			
Pr	1.765	2.447			
Sr	393.886	275.665			
Nd	8.123	10.623			
Sm	2.144	2.557			
Zr	55.325	80.611			
Hf	1.380	1.986			
Eu	0.700	0.777			
Gd	2.315	2.563			
Tb	0.410	0.469			
Dy	2.457	2.836			
Y	12.553	14.524			
Ho	0.534	0.609			
Er	1.561	1.713			
Tm	0.219	0.251			
Yb	1.484	1.651			
Lu	0.21824	0.24415			

Source Compositions
[Input Slab compositions] [Input slab MwP composition]

Element	SlbP X(SlbP)	Slab X(DIKE)	Slab X(AOC)	Slab X(SED)	MwP X(MwP)	PM (S&McD)	DMM (W&H)	DMM (Salt&Str)
SiO2			51.15	41.28			44.71	
TiO2			1.27	0.41			0.13	
Al2O3			16.00	8.38			3.98	
Fe2O3			9.00	4.97			8.9998	
MgO			7.50	1.75			38.73	
CaO			12.00	16.86			3.17	
Na2O			2.75	1.53			0.13	
K2O			0.13	1.34			0.006	
SUM			99.80	76.53			99.8558	
Rb	0.088	13.7	13.70	83.70	0.05	0.635	0.05	0.088
Ba	1.2	15.6	15.60	786.00	0.563	6.989	0.563	1.2
Th	0.0137	0.173	0.17	8.10	0.0079	0.085	0.0079	0.0137
U	0.0047	0.39	0.39	1.73	0.0032	0.021	0.0032	0.0047
Nb	0.21	2.89	2.89	9.42	0.1485	0.713	0.1485	0.21
Ta	0.0138	0.21	0.21	0.70	0.0096	0.041	0.0096	0.0138
K	60	5147	5147.00	18346.28	80	250	80	60
La	0.234	3.4	3.40	29.10	0.192	0.687	0.192	0.234
Ce	0.772	11.4	11.40	57.60	0.55	1.775	0.55	0.772
Pb	0.0232	0.437	0.44	21.20	0.018	0.08	0.018	0.0232
Pr	0.131	2.06	2.06	7.15	0.107	0.276	0.107	0.131
Sr	9.8	110	110.00	302.00	7.664	21.1	7.664	9.8
Nd	0.713	11.3	11.30	27.60	0.581	1.354	0.581	0.713
Sm	0.27	3.95	3.95	6.00	0.239	0.444	0.239	0.27
Zr	7.94	112	112.00	129.00	5.082	11.2	5.082	7.94
Hf	0.199	3.07	3.07	3.42	0.157	0.309	0.157	0.199
Eu	0.107	1.34	1.34	1.37	0.096	0.168	0.096	0.107
Gd	0.395	5.55	5.55	5.81	0.358	0.596	0.358	0.395
Tb	0.075	1.01	1.01	0.92	0.07	0.108	0.07	0.075
Dy	0.531	6.56	6.56	5.43	0.505	0.737	0.505	0.531
Y	3.256	40.7	40.70	33.30	3.2	4.55	3.2	3.256
Ho	0.122	1.43	1.43	1.10	0.115	0.164	0.115	0.122
Er	0.371	4.09	4.09	3.09	0.348	0.48	0.348	0.371
Tm	0.06	0.617	0.62		0.055	0.074	0.055	0.06
Yb	0.401	4.02	4.02	3.01	0.365	0.493	0.365	0.401
Lu	0.063	0.636	0.64	0.46	0.058	0.074	0.058	0.063

Figure S2 Data input fields for compositions of target magma and subducting materials.

In addition, we input the minimum (MIN) and maximum (MAX) values and the calculation step (STEP) of each parameter are set in the AUTO-FIT PARAMETERS boxes in the [CONTROL PANEL] worksheet (Figure S3). The calculations use random numbers generated automatically by the computer based on the Monte Carlo calculations. Once the ABS5 obtained a best-fit result, the result would be automatically saved in the [SUMMARY] worksheet.

AUTO-FIT PARAMETERS ==========

PARAM.	MIN	MAX	STEP	TIMES
P(Gpa)	3.0	5.5	0.1	26
# SLAB LIQ. FRACTIONS & %R				
Fliq(SED)	0.00	0.50	0.05	11
Fliq(DMM)	0.00	0.30	0.05	7
%R slab	60	180	10	13
# ZONE REFINING				
n(PERID)	0.0	0.0	1	1
# SOURCE PERID DEPLETION				
%MORBext.	0.0	0.0	0.5	1
# LIQUID FLUX OPEN SYSTEM MELTING				
P (Gpa)	1.0	2.5	0.1	16
T(C)	1100	1300	10	21
Fslb liq.%	3.0	10.0	0.5	15

Rand max.#	Fit#	Cycle	%Done	Max
5,000,000	8	1222704	24.45	98,378,280

Figure S3 Auto-fit parameters and fitting windows used for Monte Carlo calculations

2. ANALYTICAL DATA AND MODELING RESULTS

Insert Tables S1–S6.

3. REFERENCES CITED

Balcaen, L., De Schrijver, I., Moens, L., and Vanhaecke, F., 2005, Determination of the $^{87}Sr/^{86}Sr$ isotope ratio in USGS silicate reference materials by multi-collector ICP-mass spectrometry: International Journal of Mass Spectrometry, v. 242, p. 251–255, https://doi.org/10.1016/j.ijms.2004.10.025.

Blichert-Toft, J., and Albarede, F., 1997, The Lu-Hf isotope geochemistry of chondrites and the evolution of the mantle-crust system: Earth and Planetary Science Letters, v. 148, p. 243–258, https://doi.org/10.1016/S0012-821X(97)00040-X.

Black, L.P., Kamo, S.L., Allen, C.M., Aleinikoff, J.N., Davis, D.W., Korsch, R.J., and Foudoulis, C., 2003, TEMORA 1: A new zircon standard for Phanerozoic U-Pb geochronology: Chemical Geology, v. 200, p. 155–170, https://doi.org/10.1016/S0009-2541(03)00165-7.

Chu, Z.Y., Chen, F.K., Yang, Y.H., and Guo, J.H., 2009, Precise determination of Sm, Nd concentrations and Nd isotopic compositions at the nanogram level in geological samples by thermal ionization mass spectrometry: Journal of Analytical Atomic Spectrometry, v. 24, p. 1534–1544, https://doi.org/10.1039/b904047a.

Gao, S., Liu, X.M., Yuan, H.L., Hattendorf, B., Gunther, D., Chen, L., and Hu, S.H., 2002, Determination of forty two major and trace elements in USGS and NIST SRM glasses by laser ablation-inductively coupled plasma-mass spectrometry: Geostandards Newsletter, v. 26, p. 181–196, https://doi.org/10.1111/j.1751-908X.2002.tb00886.x.

Herzberg, C., Asimow, P.D., Arndt, N., Niu, Y., Lesher, C.M., Fitton, J.G., Cheadle, M.J., and Saunders, A.D., 2007, Temperatures in ambient mantle and plumes: Constraints from basalts, picrites, and komatiites: Geochemistry Geophysics Geosystems, v. 8, https://doi.org/10.1029/2006GC001390.

Huang, F., Chen, J.-L., Xu, J.-F., Wang, B.-D., and Li, J., 2015, Os–Nd–Sr isotopes in Miocene ultrapotassic rocks of southern Tibet: Partial melting of a pyroxenite-bearing lithospheric mantle?: Geochimica et Cosmochimica Acta, v. 163, p. 279–298, https://doi.org/10.1016/j.gca.2015.04.053.

Huang, F., Xu, J.F., Zeng, Y.C., Chen, J.L., Wang, B.D., Yu, H.X., Chen, L., Huang, W.L., and Tan, R.Y., 2017, Slab Breakoff of the Neo-Tethys Ocean in the Lhasa Terrane Inferred From Contemporaneous Melting of the Mantle and Crust: Geochemistry Geophysics Geosystems, v. 18, p. 4074–4095, https://doi.org/10.1002/2017GC007039.

Ireland, T.R., and Williams, I.S., 2003, Considerations in zircon geochronology by SIMS: Reviews in Mineralogy and Geochemistry, v. 53, p. 215–241, https://doi.org/10.2113/0530215.

Jackson, S.E., Pearson, N.J., Griffin, W.L., and Belousova, E.A., 2004, The application of laser ablation-inductively coupled plasma-mass spectrometry to in situ U-Pb zircon geochronology: Chemical Geology, v. 211, p. 47–69, https://doi.org/10.1016/j.chemgeo.2004.06.017.

Jacobsen, S.B., and Wasserburg, G.J., 1980, Sm-Nd Isotopic Evolution of Chondrites: Earth and Planetary Science Letters, v. 50, p. 139–155, https://doi.org/10.1016/0012-821X(80)90125-9.

Katz, R.F., Spiegelman, M., and Langmuir, C.H., 2003, A new parameterization of hydrous mantle melting: Geochemistry Geophysics Geosystems, v. 4, https://doi.org/10.1029/2002GC000433.

Kimura, J.-I., 2017, Modeling chemical geodynamics of subduction zones using the Arc Basalt Simulator version 5: Geosphere, v. 13, p. 992–1025, https://doi.org/10.1130/GES01468.1.
Kimura, J.I., and Ariskin, A.A., 2014, Calculation of water-bearing primary basalt and estimation of source mantle conditions beneath arcs: PRIMACALC2 model for WINDOWS: Geochemistry Geophysics Geosystems, v. 15, p. 1494–1514, https://doi.org/10.1002/2014GC005329.
Li, X., Tang, G., Gong, B., Yang, Y., Hou, K., Hu, Z., Li, Q., Liu, Y., and Li, W., 2013, Qinghu zircon: A working reference for microbeam analysis of U-Pb age and Hf and O isotopes: Chinese Science Bulletin, v. 58, p. 4647–4654, https://doi.org/10.1007/s11434-013-5932-x.
Li, X.H., Liu, Y., Li, Q.L., Guo, C.H., and Chamberlain, K.R., 2009, Precise determination of Phanerozoic zircon Pb/Pb age by multicollector SIMS without external standardization: Geochemistry Geophysics Geosystems, v. 10, https://doi.org/10.1029/2009gc002400.
Li, X.-H., Long, W.-G., Li, Q.-L., Liu, Y., Zheng, Y.-F., Yang, Y.-H., Chamberlain, K.R., Wan, D.-F., Guo, C.-H., Wang, X.-C., and Tao, H., 2010, Penglai Zircon Megacrysts: A Potential New Working Reference Material for Microbeam Determination of Hf–O Isotopes and U–Pb Age: Geostandards and Geoanalytical Research, v. 34, p. 117–134, https://doi.org/10.1111/j.1751-908X.2010.00036.x.
Liu, Y.S., Hu, Z.C., Gao, S., Gunther, D., Xu, J., Gao, C.G., and Chen, H.H., 2008, In situ analysis of major and trace elements of anhydrous minerals by LA-ICP-MS without applying an internal standard: Chemical Geology, v. 257, p. 34–43, https://doi.org/10.1016/j.chemgeo.2008.08.004.
Ludwing, K., 2003, User's manual for Isoplot 3.00: a geochronological toolkit for Microsoft Excel. Special Publication, Berkeley Geochronology Center, p. 1–70.
Lugmair, G.W., and Marti, K., 1978, Lunar Initial 143Nd-144Nd Differential Evolution of Lunar Crust and Mantle: Earth and Planetary Science Letters, v. 39, p. 349–357, https://doi.org/10.1016/0012-821X(78)90021-3.
Morel, M.L.A., Nebel, O., Nebel-Jacobsen, Y.J., Miller, J.S., and Vroon, P.Z., 2008, Hafnium isotope characterization of the GJ-1 zircon reference material by solution and laser-ablation MC-ICPMS: Chemical Geology, v. 255, p. 231–235, https://doi.org/10.1016/j.chemgeo.2008.06.040.
Plank, T., 2014, The Chemical Composition of Subducting Sediments, *in* Holland, H.D., and Turekian, K.K., eds., Treatise on Geochemistry (Second Edition): Oxford, Elsevier, p. 607–629, https://doi.org/10.1016/B978-0-08-095975-7.00319-3.
Sláma, J., Kosler, J., Condon, D.J., Crowley, J.L., Gerdes, A., Hanchar, J.M., Horstwood, M.S.A., Morris, G.A., Nasdala, L., Norberg, N., Schaltegger, U., Schoene, B., Tubrett, M.N., and Whitehouse, M.J., 2008, Plesovice zircon-A new natural reference material for U-Pb and Hf isotopic microanalysis: Chemical Geology, v. 249, p. 1–35, https://doi.org/10.1016/j.chemgeo.2007.11.005.
Söderlund, U., Patchett, J.P., Vervoort, J.D., and Isachsen, C.E., 2004, The Lu-176 decay constant determined by Lu-Hf and U-Pb isotope systematics of Precambrian mafic intrusions: Earth and Planetary Science Letters, v. 219, p. 311–324, https://doi.org/10.1016/S0012-821X(04)00012-3.
Stacey, J.S., and Kramers, J.D., 1975, Approximation of terrestrial lead isotope evolution by a 2-stage model: Earth and Planetary Science Letters, v. 26, p. 207–221, https://doi.org/10.1016/0012-821X(75)90088-6.

Steiger, R.H., and Jager, E., 1977, Subcommission on Geochronology: Convention on Use of Decay Constants in Geochronology and Cosmochronology: Earth and Planetary Science Letters, v. 36, p. 359–362, https://doi.org/10.1016/0012-821X(77)90060-7.

Whitehouse, M.J., Claesson, S., Sunde, T., and Vestin, J., 1997, Ion microprobe U-Pb zircon geochronology and correlation of Archaean gneisses from the Lewisian Complex of Gruinard Bay, northwestern Scotland: Geochimica et Cosmochimica Acta, v. 61, p. 4429–4438, https://doi.org/10.1016/S0016-7037(97)00251-2.

Workman, R.K., and Hart, S.R., 2005, Major and trace element composition of the depleted MORB mantle (DMM): Earth and Planetary Science Letters, v. 231, p. 53–72, https://doi.org/10.1016/j.epsl.2004.12.005.

Wu, F.Y., Yang, Y.H., Xie, L.W., Yang, J.H., and Xu, P., 2006, Hf isotopic compositions of the standard zircons and baddeleyites used in U-Pb geochronology: Chemical Geology, v. 234, p. 105–126, https://doi.org/10.1016/j.chemgeo.2006.05.003.

Yuan, H.L., Gao, S., Dai, M.N., Zong, C.L., Gunther, D., Fontaine, G.H., Liu, X.M., and Diwu, C., 2008, Simultaneous determinations of U-Pb age, Hf isotopes and trace element compositions of zircon by excimer laser-ablation quadrupole and multiple-collector ICP-MS: Chemical Geology, v. 247, p. 100–118, https://doi.org/10.1016/j.chemgeo.2007.10.003.

TABLE S1

TABLE S1. SIMS U-PB ZIRCON DATING RESULTS FOR DAZI MAFIC ROCKS

Sample spot	U/ppm	Th/ppm	Pb/ppm	Th/U	f_{206}%	Ratios					Age			
						$^{207}Pb/^{235}U$	±1σ %	$^{206}Pb/^{238}U$	±1σ %	ρ	$^{207}Pb/^{235}U$	±1σ	$^{207}Pb/^{235}U$	±1σ
10LKE-01@1	427	183	5	0.4	0.24	0.05669	4.26	0.0092	2.45	0.58	56.0	2.3	58.9	1.4
10LKE-01@2	99	61	76	0.6	0.04	16.69392	2.43	0.5571	2.40	0.99	2917.4	23.5	2854.5	55.6
10LKE-01@3	234	79	22	0.3	1.38	0.63273	3.10	0.0800	2.40	0.77	497.8	12.3	496.3	11.5
10LKE-01@4	239	133	3	0.6	0.78	0.05562	5.24	0.0087	2.48	0.47	55.0	2.8	56.1	1.4
10LKE-01@5	259	159	3	0.6	0.01	0.06008	4.12	0.0089	2.50	0.61	59.2	2.4	57.1	1.4
10LKE-01@6	157	88	5	0.6	0.20	0.16854	4.33	0.0248	2.41	0.56	158.2	6.4	157.8	3.8
10LKE-01@7	111	88	1	0.8	1.38	0.05961	6.61	0.0092	2.58	0.58	58.8	3.8	59.0	1.5
10LKE-01@8	255	189	87	0.7	0.05	3.42997	2.44	0.2577	2.40	0.98	1511.3	19.4	1477.8	31.8
10LKE-01@9	177	148	6	0.8	0.65	0.15422	5.27	0.0241	2.42	0.46	145.6	7.2	153.7	3.7
11DZ-20@1	124	122	2	1.0	1.58	0.06106	14.50	0.0091	2.01	0.14	60.2	8.5	58.4	1.2
11DZ-20@2	175	250	126	1.4	0.05	10.40803	1.61	0.4632	1.52	0.95	2471.8	15.0	2453.8	31.1
11DZ-20@3	132	111	2	0.8	4.02	0.07929	19.52	0.0087	2.28	0.12	77.5	14.7	55.8	1.3
11DZ-20@4	77	44	1	0.6	0.02	0.07089	14.44	0.0094	2.23	0.15	69.5	9.7	60.2	1.3
11DZ-20@5	189	199	2	1.1	1.27	0.05037	13.85	0.0085	2.01	0.15	49.9	6.8	54.4	1.1
11DZ-20@6	182	148	2	0.8	2.99	0.04364	26.95	0.0085	1.82	0.07	43.4	11.5	54.8	1.0
11DZ-20@7	138	143	2	1.0	1.30	0.05997	17.25	0.0090	2.04	0.12	59.1	10.0	58.0	1.2
11DZ-20@8	112	69	1	0.6	1.03	0.05752	15.60	0.0092	2.07	0.13	56.8	8.7	59.2	1.2
11DZ-20@9	158	165	2	1.0	1.88	0.05009	21.08	0.0089	2.36	0.11	49.6	10.3	56.8	1.3
11DZ-20@10	225	211	3	0.9	0.94	0.07132	10.43	0.0088	1.84	0.18	70.0	7.1	56.6	1.0
11DZ-20@11	151	119	2	0.8	2.23	0.04554	22.91	0.0093	1.99	0.09	45.2	10.2	59.4	1.2
11DZ-20@12	194	198	2	1.0	1.89	0.04372	18.94	0.0085	1.92	0.10	43.4	8.1	54.7	1.0
11DZ-20@13	113	82	1	0.7	2.72	0.04514	29.05	0.0087	2.53	0.09	44.8	12.8	56.0	1.4
11DZ-20@14	352	283	4	0.8	0.34	0.06179	7.62	0.0087	2.25	0.29	60.9	4.5	55.9	1.3
11DZ-20@15	112	75	1	0.7	1.58	0.05415	24.65	0.0092	1.76	0.07	53.5	12.9	59.2	1.0
13DZ-09@01	99	49	1	0.5	1.34	0.06441	4.47	0.0094	3.43	0.77	63.4	2.7	60.4	2.1
13DZ-09@02	131	65	2	0.5	0.88	0.06903	4.22	0.0094	3.41	0.81	67.8	2.8	60.4	2.1
13DZ-09@03	80	65	1	0.8	0.90	0.06079	5.57	0.0086	3.45	0.62	59.9	3.2	55.1	1.9
13DZ-09@04	421	371	5	0.9	0.59	0.06320	3.72	0.0096	3.34	0.90	62.2	2.2	61.8	2.1
13DZ-09@05	121	57	1	0.5	0.51	0.06454	4.26	0.0093	3.39	0.80	63.5	2.6	59.6	2.0
13DZ-09@06	142	124	2	0.9	2.93	0.08202	4.24	0.0093	3.38	0.80	80.0	3.3	59.6	2.0
13DZ-09@07	260	136	3	0.5	4.76	0.06727	3.97	0.0091	3.44	0.87	66.1	2.5	58.3	2.0
13DZ-09@08	75	58	1	0.8	1.18	0.06351	4.83	0.0086	3.52	0.73	62.5	2.9	55.0	1.9
13DZ-09@09	80	55	1	0.7	1.04	0.06970	4.64	0.0095	3.43	0.74	68.4	3.1	60.7	2.1
13DZ-09@10	106	66	1	0.6	0.77	0.06769	4.40	0.0096	3.45	0.78	66.5	2.8	61.5	2.1
13DZ-09@11	123	133	1	1.1	0.74	0.06158	4.56	0.0087	3.36	0.74	60.7	2.7	55.9	1.9
13DZ-09@12	157	132	2	0.8	6.60	0.12036	5.71	0.0091	3.39	0.59	115.4	6.2	58.4	2.0
13DZ-09@13	1226	1342	37	1.1	0.33	0.15016	3.58	0.0212	3.33	0.93	142.1	4.8	134.9	4.4
13DZ-09@14	422	412	12	1.0	0.65	0.14879	3.57	0.0207	3.33	0.93	140.8	4.7	132.3	4.4
13DZ-09@15	170	84	2	0.5	1.98	0.07575	3.97	0.0093	3.37	0.85	74.1	2.8	59.5	2.0
13DZ-09@16	1247	1537	38	1.2	0.31	0.14537	3.39	0.0206	3.33	0.98	137.8	4.4	131.6	4.3
13DZ-09@17	295	370	9	1.3	0.48	0.14243	3.61	0.0206	3.35	0.93	135.2	4.6	131.6	4.4
13DZ-09@18	863	517	23	0.6	0.40	0.15140	3.42	0.0213	3.33	0.97	143.1	4.6	135.7	4.5
13DZ-09@19	161	108	4	0.7	1.77	0.17303	4.05	0.0205	3.37	0.83	162.0	6.1	130.5	4.4
13DZ-09@20	530	482	15	0.9	0.32	0.14335	3.56	0.0207	3.33	0.94	136.0	4.5	132.4	4.4
13DZ-11@01	234	238	3	1.0	0.93	0.06422	4.54	0.0094	3.37	0.74	63.2	2.8	60.6	2.0
13DZ-11@02	148	86	2	0.6	1.19	0.06696	4.09	0.0094	3.37	0.82	65.8	2.6	60.2	2.0
13DZ-11@03	177	98	2	0.6	0.68	0.06397	4.16	0.0092	3.40	0.82	63.0	2.5	58.9	2.0
13DZ-11@04	151	147	2	1.0	2.96	0.08170	4.89	0.0088	3.52	0.72	79.7	3.8	56.4	2.0
13DZ-11@05	172	191	2	1.1	1.05	0.05812	4.18	0.0084	3.44	0.82	57.4	2.3	54.0	1.9
13DZ-11@06	147	141	2	1.0	1.11	0.05633	4.32	0.0082	3.45	0.80	55.6	2.3	52.9	1.8
13DZ-11@07	114	95	1	0.8	1.49	0.06883	4.56	0.0088	3.44	0.75	67.6	3.0	56.5	1.9
13DZ-11@08	344	216	4	0.6	0.41	0.06497	3.75	0.0095	3.37	0.90	63.9	2.3	60.8	2.0

TABLE S2

TABLE S2. LA-ICP-MS U-PB ZIRCON DATING RESULTS FOR DAZI MAFIC SAMPLES

Sample spot	U/ppm	Th/ppm	Pb/ppm	Th/U	Ratios					Age			
					$^{207}Pb/^{235}U$	±1σ	$^{206}Pb/^{238}U$	±1σ	ρ	$^{207}Pb/^{235}U$	±1σ	$^{206}Pb/^{238}U$	±1σ
11DZ-06-01	1855	3405	28	1.8	0.0610	0.0046	0.0091	0.0002	0.28	60.1	4.4	58.3	1.2
11DZ-06-02	132	90	2	0.7	0.0614	0.0274	0.0088	0.0006	0.14	60.5	26.2	56.6	3.6
11DZ-06-03	554	440	7	0.8	0.0618	0.0081	0.0090	0.0003	0.28	60.8	7.7	57.5	2.1
11DZ-06-04	208	207	2	1.0	0.0617	0.0187	0.0089	0.0007	0.27	60.7	17.9	57.4	4.7
11DZ-06-05	142	93	2	0.7	0.0622	0.0163	0.0089	0.0005	0.21	61.2	15.6	57.2	3.2
11DZ-06-06	267	239	3	0.9	0.0617	0.0102	0.0091	0.0005	0.35	60.8	9.7	58.3	3.3
11DZ-06-07	119	73	1	0.6	0.0594	0.0314	0.0089	0.0006	0.14	58.6	30.1	56.9	4.1
11DZ-06-08	139	98	2	0.7	0.0606	0.0184	0.0090	0.0006	0.21	59.8	17.6	57.6	3.7
11DZ-06-09	117	63	1	0.5	0.0626	0.0189	0.0088	0.0004	0.16	61.7	18.1	56.4	2.8
11DZ-06-10	68	53	1	0.8	0.0606	0.0265	0.0086	0.0005	0.13	59.7	25.4	55.5	3.1
11DZ-06-11	115	76	1	0.7	0.0575	0.0163	0.0087	0.0004	0.17	56.8	15.6	55.7	2.7
11DZ-06-12	200	144	2	0.7	0.0591	0.0100	0.0089	0.0003	0.22	58.3	9.6	57.3	2.1
11DZ-06-13	107	73	1	0.7	0.0601	0.0193	0.0088	0.0007	0.23	59.2	18.5	56.4	4.2
11DZ-06-14	112	71	1	0.6	0.0582	0.0336	0.0089	0.0008	0.16	57.4	32.2	57.0	5.2
11DZ-06-15	84	36	13	0.4	1.1900	0.0607	0.1287	0.0020	0.31	796.0	28.2	780.7	11.6
11DZ-06-16	144	97	2	0.7	0.0625	0.0096	0.0091	0.0004	0.32	61.5	9.2	58.1	2.8
11DZ-06-17	148	98	2	0.7	0.0583	0.0193	0.0089	0.0005	0.17	57.6	18.5	57.3	3.3
11DZ-06-18	244	281	3	1.2	0.0628	0.0161	0.0091	0.0007	0.29	61.9	15.4	58.4	4.3
11DZ-06-19	106	64	1	0.6	0.0587	0.0324	0.0089	0.0009	0.19	57.9	31.1	56.9	5.9
11DZ-06-20	223	58	2	0.3	0.0605	0.0089	0.0091	0.0003	0.20	59.6	8.6	58.1	1.7
11DZ-06-21	127	77	1	0.6	0.0591	0.0118	0.0090	0.0004	0.23	58.3	11.3	57.9	2.7
11DZ-06-22	186	222	2	1.2	0.0631	0.0151	0.0089	0.0007	0.33	62.1	14.5	57.3	4.6
11DZ-10-01	108	97	1	0.9	0.0573	0.0184	0.0089	0.0006	0.22	56.6	17.7	57.2	4.1
11DZ-10-02	66	40	1	0.6	0.0621	0.0231	0.0089	0.0005	0.15	61.2	22.1	57.0	3.3
11DZ-10-03	227	217	3	1.0	0.0628	0.0082	0.0089	0.0003	0.26	61.9	7.9	56.9	1.9
11DZ-10-04	179	177	2	1.0	0.0591	0.0114	0.0089	0.0004	0.24	58.3	10.9	57.2	2.7
11DZ-10-05	226	211	3	0.9	0.0635	0.0142	0.0089	0.0004	0.20	62.5	13.6	56.9	2.5
11DZ-10-06	156	112	2	0.7	0.0617	0.0125	0.0089	0.0004	0.21	60.8	11.9	57.3	2.5
11DZ-10-07	686	826	26	1.2	0.2041	0.0096	0.0276	0.0005	0.35	188.6	8.1	175.4	2.9
11DZ-10-08	163	138	2	0.9	0.0653	0.0261	0.0091	0.0005	0.14	64.2	24.9	58.3	3.2
11DZ-10-09	190	165	2	0.9	0.0534	0.0174	0.0085	0.0004	0.13	52.8	16.8	54.7	2.4
11DZ-10-10	113	62	1	0.5	0.0637	0.0171	0.0093	0.0007	0.27	62.7	16.4	59.5	4.3
11DZ-10-11	148	103	2	0.7	0.0616	0.0101	0.0092	0.0006	0.41	60.7	9.6	58.9	4.0
11DZ-10-12	358	476	5	1.3	0.0621	0.0244	0.0088	0.0008	0.22	61.2	23.3	56.8	4.9
11DZ-10-13	294	225	17	0.8	0.3616	0.0169	0.0459	0.0007	0.32	313.4	12.6	289.2	4.2
11DZ-10-14	147	149	5	1.0	0.1796	0.0185	0.0260	0.0007	0.25	167.7	15.9	165.5	4.2
11DZ-10-15	158	127	2	0.8	0.0668	0.0149	0.0092	0.0003	0.14	65.7	14.2	59.3	1.9
11DZ-10-16	120	77	1	0.6	0.0657	0.0235	0.0093	0.0006	0.19	64.7	22.4	59.7	4.1
11DZ-10-17	89	57	1	0.6	0.0616	0.0381	0.0092	0.0006	0.10	60.7	36.5	59.1	3.7
11DZ-10-18	167	102	2	0.6	0.0649	0.0179	0.0091	0.0005	0.19	63.9	17.1	58.7	3.1
11DZ-10-19	111	72	1	0.6	0.0594	0.0155	0.0087	0.0005	0.21	58.5	14.9	55.6	3.1
11DZ-10-20	158	143	2	0.9	0.0562	0.0159	0.0086	0.0004	0.16	55.5	15.3	55.1	2.5
11DZ-10-21	248	156	3	0.6	0.0579	0.0083	0.0088	0.0003	0.23	57.2	7.9	56.7	1.9
11DZ-10-22	130	117	1	0.9	0.0640	0.0107	0.0090	0.0005	0.30	63.0	10.2	57.5	2.9
11DZ-10-23	143	140	2	1.0	0.0650	0.0115	0.0093	0.0003	0.16	63.9	11.0	59.9	1.6
11DZ-21-01	785	506	9	0.6	0.0614	0.0080	0.0090	0.0002	0.21	60.5	7.6	57.7	1.6
11DZ-21-02	294	350	4	1.2	0.0611	0.0303	0.0090	0.0007	0.16	60.2	29.0	57.8	4.6
11DZ-21-03	151	120	2	0.8	0.0522	0.0262	0.0083	0.0007	0.16	51.7	25.3	53.2	4.4
11DZ-21-04	462	419	5	0.9	0.0561	0.0234	0.0089	0.0009	0.24	55.4	22.5	56.9	5.7
11DZ-21-05	333	308	5	0.9	0.0594	0.0197	0.0087	0.0006	0.21	58.6	18.9	55.6	3.9
11DZ-21-06	91	70	1	0.8	0.0528	0.0000	0.0085	0.0004	0.31	52.3	3.1	54.8	2.3
11DZ-21-07	104	51	1	0.5	0.0619	0.0395	0.0087	0.0007	0.12	61.0	37.8	55.7	4.3
11DZ-21-08	82	40	1	0.5	0.0648	0.0208	0.0090	0.0004	0.15	63.8	19.9	57.8	2.7
11DZ-21-09	130	167	28	1.3	1.3672	0.0757	0.1476	0.0022	0.27	875.0	32.5	887.6	12.6
11DZ-23-01	98	94	1	1.0	0.0590	0.0241	0.0089	0.0004	0.12	58.2	23.1	57.4	2.7
11DZ-23-02	101	98	1	1.0	0.0581	0.0216	0.0088	0.0008	0.24	57.3	20.7	56.2	4.9
11DZ-23-03	97	62	1	0.6	0.0651	0.0261	0.0092	0.0005	0.14	64.0	24.9	59.0	3.2
11DZ-23-04	58	40	1	0.7	0.0631	0.0298	0.0090	0.0005	0.12	62.1	28.4	57.5	3.3
11DZ-23-05	120	105	1	0.9	0.0561	0.0317	0.0088	0.0008	0.15	55.5	30.5	56.5	4.8
11DZ-23-06	113	115	1	1.0	0.0658	0.0288	0.0092	0.0008	0.19	64.8	27.5	58.8	4.9
13DZ-10-01	93	80	1	0.9	0.0562	0.0246	0.0088	0.0011	0.28	55.5	23.7	56.3	6.8
13DZ-10-02	172	234	2	1.4	0.0637	0.0242	0.0090	0.0009	0.26	62.7	23.1	57.5	5.7
13DZ-10-03	61	54	1	0.9	0.0566	0.0311	0.0092	0.0009	0.17	56.0	29.9	59.1	5.5
13DZ-10-04	92	70	1	0.8	0.0578	0.0131	0.0092	0.0006	0.29	57.0	12.6	59.3	3.9
13DZ-10-05	89	89	1	1.0	0.0629	0.0183	0.0092	0.0003	0.12	61.9	17.4	58.9	2.1
13DZ-10-06	68	45	1	0.7	0.0636	0.0301	0.0093	0.0005	0.12	62.6	28.7	59.5	3.5
13DZ-10-07	88	76	1	0.9	0.0601	0.0073	0.0090	0.0003	0.28	59.2	7.0	57.8	1.9
13DZ-10-08	70	52	1	0.7	0.0628	0.0188	0.0091	0.0004	0.14	61.9	18.0	58.2	2.5
13DZ-10-09	78	60	1	0.8	0.0634	0.0165	0.0090	0.0003	0.15	62.4	15.8	57.5	2.2
13DZ-10-10	68	59	1	0.9	0.0629	0.0171	0.0087	0.0004	0.17	61.9	16.3	56.2	2.6
13DZ-10-11	198	138	2	0.7	0.0591	0.0065	0.0090	0.0002	0.23	58.3	6.2	57.6	1.5
13DZ-10-12	69	58	1	0.8	0.0563	0.0174	0.0088	0.0004	0.13	55.6	16.7	56.5	2.3
13DZ-10-13	94	103	1	1.1	0.0605	0.0054	0.0087	0.0004	0.49	59.7	5.2	56.1	2.4
13DZ-10-14	101	111	1	1.1	0.0610	0.0188	0.0088	0.0004	0.14	60.1	18.0	56.8	2.3
13DZ-10-15	157	77	2	0.5	0.0595	0.0074	0.0090	0.0003	0.27	58.7	7.1	57.5	1.9
13DZ-10-16	79	63	1	0.8	0.0604	0.0087	0.0087	0.0003	0.25	59.6	8.4	55.6	2.0
13DZ-15-01	152	136	2	0.9	0.0611	0.0288	0.0091	0.0008	0.18	60.2	27.6	58.2	4.8
13DZ-15-02	216	115	3	0.5	0.0607	0.0129	0.0090	0.0006	0.31	59.9	12.4	57.6	3.8
13DZ-15-03	193	110	2	0.6	0.0621	0.0218	0.0089	0.0006	0.18	61.2	20.8	57.0	3.6
13DZ-15-04	209	165	2	0.8	0.0589	0.0112	0.0090	0.0004	0.22	58.1	10.7	57.6	2.4
13DZ-15-05	137	89	2	0.7	0.0610	0.0163	0.0089	0.0004	0.17	60.1	15.6	57.0	2.5

TABLE S2

13DZ-15-06	172	112	2	0.7	0.0593	0.0132	0.0089	0.0003	0.16	58.5	12.7	56.9	2.0
13DZ-15-07	161	116	2	0.7	0.0590	0.0100	0.0088	0.0005	0.35	58.2	9.5	56.6	3.3
13DZ-15-08	106	158	1	1.5	0.0572	0.0021	0.0088	0.0001	0.44	56.4	2.0	56.3	0.9
13DZ-15-09	313	315	4	1.0	0.0595	0.0088	0.0088	0.0004	0.33	58.7	8.5	56.7	2.8
13DZ-15-10	412	225	5	0.5	0.0637	0.0051	0.0092	0.0002	0.27	62.7	4.8	59.2	1.3
13DZ-15-11	256	224	4	0.9	0.0610	0.0084	0.0091	0.0008	0.64	60.1	8.1	58.6	5.2
13DZ-15-12	310	292	4	0.9	0.0629	0.0105	0.0091	0.0004	0.27	61.9	10.1	58.4	2.6
13DZ-15-13	1100	781	14	0.7	0.0577	0.0069	0.0087	0.0001	0.13	57.0	6.7	56.1	0.9
13DZ-15-14	1712	1835	24	1.1	0.0621	0.0074	0.0087	0.0003	0.25	61.1	7.1	56.1	1.7
13DZ-15-15	108	74	1	0.7	0.0591	0.0160	0.0090	0.0006	0.27	58.3	15.3	57.5	4.1
13DZ-15-16	159	181	2	1.1	0.0630	0.0132	0.0090	0.0006	0.32	62.0	12.6	57.6	3.9

TABLE S3

TABLE S3. HF ISOTOPIC RESULTS OF DAZI MAFIC ROCKS

Sample spot	Age	$^{176}Yb/^{177}Hf$	±1σ	$^{176}Lu/^{177}Hf$	±1σ	$^{176}Hf/^{177}Hf$	±1σ	$^{176}Hf/^{177}Hf_i$	$\varepsilon_{Hf}(t)$
11DZ-06-03	57.5	0.032652	0.001303	0.001101	0.000036	0.283020	0.000087	0.283019	10.0
11DZ-06-06	58.3	0.044606	0.000609	0.001460	0.000013	0.283020	0.000074	0.283018	10.0
11DZ-06-16	58.1	0.022067	0.000368	0.000755	0.000008	0.283013	0.000061	0.283012	9.8
11DZ-06-17	57.3	0.024119	0.000606	0.000839	0.000020	0.283085	0.000050	0.283084	12.3
11DZ-06-18	58.4	0.037508	0.000459	0.001307	0.000015	0.283043	0.000039	0.283041	10.8
11DZ-06-22	57.3	0.044982	0.000444	0.001481	0.000014	0.283047	0.000025	0.283045	10.9
11DZ-10-01	57.2	0.050150	0.007083	0.001423	0.000271	0.283056	0.000015	0.283054	11.2
11DZ-10-02	57.0	0.033637	0.000246	0.000975	0.000012	0.282995	0.000015	0.282994	9.1
11DZ-10-03	56.9	0.056631	0.000529	0.001846	0.000016	0.283009	0.000013	0.283007	9.6
11DZ-10-04	57.2	0.043901	0.000642	0.001462	0.000023	0.283035	0.000018	0.283033	10.5
11DZ-10-06	57.3	0.039390	0.000817	0.001321	0.000019	0.282954	0.000016	0.282953	7.7
11DZ-10-07	175.5	0.079588	0.000945	0.002718	0.000039	0.282869	0.000014	0.282860	7.0
11DZ-10-08	58.3	0.021370	0.000336	0.000766	0.000017	0.283017	0.000021	0.283016	9.9
11DZ-10-10	59.5	0.053581	0.000615	0.001747	0.000031	0.282987	0.000018	0.282985	8.8
11DZ-10-11	58.9	0.027263	0.000238	0.000981	0.000009	0.282986	0.000015	0.282985	8.8
11DZ-10-12	56.8	0.048288	0.000564	0.001868	0.000045	0.282944	0.000030	0.282942	7.3
11DZ-10-14	165.5	0.047581	0.000853	0.001597	0.000020	0.282916	0.000012	0.282912	8.6
11DZ-10-15	59.3	0.028518	0.000770	0.001105	0.000034	0.282978	0.000023	0.282977	8.6
11DZ-10-16	59.7	0.033561	0.000626	0.001097	0.000018	0.282980	0.000017	0.282979	8.6
11DZ-10-17	59.1	0.026300	0.000198	0.000885	0.000005	0.282969	0.000015	0.282968	8.2
11DZ-10-18	58.7	0.026835	0.000607	0.000900	0.000011	0.282971	0.000016	0.282970	8.3
11DZ-10-19	55.6	0.028916	0.000333	0.001114	0.000019	0.282980	0.000020	0.282979	8.5
11DZ-10-20	55.1	0.038098	0.000223	0.001402	0.000020	0.283013	0.000024	0.283012	9.7
11DZ-10-21	56.7	0.035723	0.000760	0.001196	0.000032	0.283009	0.000024	0.283007	9.6
11DZ-10-23	59.9	0.051959	0.000877	0.001592	0.000018	0.282980	0.000019	0.282979	8.6
13DZ-10-01	56.3	0.031823	0.000340	0.000916	0.000007	0.283009	0.000010	0.283008	9.6
13DZ-10-03	59.1	0.028568	0.000128	0.000857	0.000003	0.283006	0.000010	0.283005	9.5
13DZ-10-04	59.3	0.026155	0.000054	0.000775	0.000003	0.282980	0.000010	0.282979	8.6
13DZ-10-05	58.9	0.042330	0.000482	0.001259	0.000016	0.282967	0.000010	0.282966	8.1
13DZ-10-06	59.5	0.028021	0.000157	0.000834	0.000005	0.283002	0.000010	0.283001	9.4
13DZ-10-07	57.8	0.036404	0.000141	0.001105	0.000008	0.282993	0.000010	0.282992	9.1
13DZ-10-10	56.2	0.047687	0.000365	0.001605	0.000017	0.282955	0.000015	0.282953	7.6
13DZ-10-11	57.6	0.024198	0.000093	0.000707	0.000003	0.283013	0.000008	0.283012	9.8
13DZ-10-12	56.5	0.029521	0.000198	0.000843	0.000002	0.283019	0.000011	0.283018	10.0
13DZ-10-14	56.8	0.029907	0.000128	0.000880	0.000006	0.282991	0.000011	0.282990	9.0
13DZ-10-15	57.5	0.054693	0.000314	0.001663	0.000008	0.283025	0.000012	0.283023	10.1

TABLE S4-1

TABLE S4. MAJOR (WT. %), TRACE ELEMENT (PPM) AND SR-ND ISOTOPIC DATA OF DAZI MAFIC SAMPLES

Sample	10LKE-01	10LKE-03	10LKE-04	10LKE-05	11DZ-03	11DZ-04	11DZ-06	11DZ-10	11DZ-11	11DZ-12	11DZ-13	11DZ-14	11DZ-15	11DZ-16
SiO_2	46.79	49.48	49.43	49.19	51.13	55.80	53.95	58.44	54.89	53.65	51.83	51.17	52.18	51.86
TiO_2	1.06	0.96	1.04	1.08	1.00	0.95	0.79	0.92	0.83	0.89	1.36	1.05	1.00	1.04
Al_2O_3	16.38	17.89	17.94	18.34	15.61	17.05	15.12	18.03	16.42	16.85	16.96	18.78	18.37	15.36
Fe_2O_{3T}	11.26	7.38	8.73	7.05	9.70	8.49	8.31	7.54	8.37	9.26	12.39	11.20	11.09	9.35
MnO	0.19	0.13	0.12	0.13	0.14	0.13	0.11	0.10	0.16	0.13	0.21	0.18	0.17	0.13
MgO	9.73	8.20	9.39	8.16	9.44	4.63	7.45	3.46	6.45	6.47	3.96	3.66	4.26	7.70
CaO	9.16	9.33	1.98	6.05	8.23	7.86	9.18	5.53	6.68	7.42	8.52	10.19	6.49	9.28
Na_2O	2.45	2.96	3.77	4.35	3.06	2.94	2.59	3.04	4.79	2.79	2.39	2.51	3.38	3.12
K_2O	1.35	1.91	5.28	3.09	0.62	1.18	1.50	2.02	0.54	1.49	1.03	0.11	1.88	1.06
P_2O_5	0.27	0.20	0.20	0.20	0.14	0.14	0.09	0.16	0.12	0.13	0.24	0.12	0.21	0.20
LOI	0.91	1.13	1.71	1.95	0.60	0.56	0.62	0.56	0.62	0.60	0.59	0.58	0.58	0.57
Total	99.56	99.55	99.57	99.60	99.67	99.73	99.72	99.80	99.86	99.68	99.49	99.55	99.62	99.69
Mg#	65.5	71.0	70.3	71.8	68.2	54.6	66.4	50.2	62.9	60.6	41.3	41.8	45.8	64.5
Sc	30.20	32.49	34.49	34.47	27.82	23.26	29.38	12.88	26.52	24.67	32.03	34.69	15.52	25.43
V	283.5	267.2	302.0	277.1	201.0	208.9	202.7	150.8	198.6	202.3	310.3	308.8	204.6	236.1
Cr	194.90	285.80	288.00	155.90	498.20	116.80	359.40	37.25	331.00	192.00	38.00	101.80	31.22	398.60
Co	40.22	22.05	27.87	24.63	39.56	28.26	36.05	20.22	27.32	30.84	27.32	26.85	26.97	35.07
Ni	65.48	72.10	72.17	58.57	161.40	29.20	97.50	10.14	56.85	64.68	8.29	9.66	3.44	96.37
Rb	28.00	140.30	326.10	203.60	15.43	33.84	53.26	57.97	12.10	44.79	25.21	2.45	38.69	15.44
Ba	347.3	40.4	66.8	78.7	155.4	335.6	205.3	293.2	217.4	179.5	522.1	144.5	397.5	255.5
Th	3.22	0.87	0.82	0.96	2.40	4.57	4.94	3.78	3.12	1.55	1.90	1.15	1.37	2.12
U	0.93	0.33	0.32	0.43	0.66	1.40	1.58	1.03	0.93	0.49	0.53	0.33	0.41	0.59
Nb	3.83	2.46	2.39	2.83	3.03	4.18	3.16	4.23	2.89	2.13	3.70	1.59	3.32	3.19
Ta	0.27	0.17	0.15	0.19	0.23	0.35	0.32	0.35	0.25	0.19	0.23	0.12	0.33	0.26
La	17.79	8.61	6.70	8.00	10.85	13.58	10.47	12.90	10.29	6.97	13.44	6.43	11.27	14.57
Ce	38.93	18.22	15.16	18.17	23.51	28.68	22.70	27.30	21.91	15.03	29.17	14.72	24.87	31.45
Pb	6.48	8.41	6.26	7.53	8.53	9.13	5.59	6.67	188.70	9.78	5.79	4.06	5.19	5.86
Pr	5.30	2.55	2.22	2.68	3.13	3.72	2.92	3.33	2.82	1.99	3.97	2.08	3.28	4.13
Sr	305.3	390.6	186.3	450.1	521.2	406.8	329.5	282.6	589.3	242.1	872.2	549.7	439.6	663.9
Nd	23.34	11.75	10.42	12.74	13.59	15.56	12.69	13.72	11.94	8.92	17.77	9.95	14.53	17.38
Zr	80.66	59.68	58.61	70.52	85.12	123.90	96.22	87.24	85.96	62.62	85.34	59.15	80.81	93.61
Hf	2.28	1.81	1.77	2.20	2.04	2.89	2.37	2.27	2.03	1.57	2.07	1.45	1.96	2.33
Sm	5.39	2.98	2.77	3.40	3.28	3.60	3.06	3.10	2.96	2.32	4.44	2.80	3.64	3.85
Eu	1.64	0.66	0.54	1.31	1.07	1.02	0.93	0.85	0.91	0.77	1.50	0.98	1.22	1.14
Ti	5905	5338	5631	6124	5389	5364	4544	4944	4537	4765	7360	6222	5376	5954
Gd	5.18	3.32	3.13	3.90	3.30	3.42	3.06	2.98	2.99	2.38	4.52	3.19	3.52	3.38
Tb	0.81	0.60	0.56	0.69	0.56	0.61	0.56	0.49	0.51	0.41	0.79	0.57	0.57	0.56
Dy	4.78	3.87	3.71	4.48	3.27	3.73	3.38	2.78	3.14	2.41	4.66	3.60	3.18	3.08
Y	23.27	18.99	18.40	22.84	16.80	19.04	17.31	14.08	16.28	11.47	23.84	18.21	15.47	15.33
Ho	0.97	0.83	0.78	0.97	0.72	0.79	0.73	0.60	0.69	0.53	1.05	0.78	0.67	0.65
Er	2.63	2.29	2.14	2.65	1.92	2.18	2.04	1.64	1.97	1.39	2.83	2.18	1.70	1.68
Tm	0.37	0.33	0.31	0.39	0.29	0.32	0.30	0.23	0.28	0.20	0.41	0.32	0.24	0.25
Yb	2.37	2.16	1.99	2.51	1.79	2.17	1.96	1.56	1.80	1.31	2.67	2.09	1.55	1.63
Lu	0.36	0.32	0.32	0.38	0.27	0.33	0.29	0.23	0.28	0.20	0.40	0.32	0.23	0.24
$^{87}Rb/^{86}Sr$	0.27				0.09	0.24	0.47	0.59	0.06	0.54	0.08	0.01	0.25	0.07
$^{87}Sr/^{86}Sr$	0.704677				0.704650	0.704650	0.704566	0.705035	0.704571	0.705119	0.704544	0.704406	0.704708	0.704253
1σ	0.000007				0.000007	0.000010	0.000005	0.000008	0.000004	0.000003	0.000003	0.000003	0.000003	0.000003
$^{87}Sr/^{86}Sr_i$	0.704463				0.704581	0.704456	0.704187	0.704555	0.704523	0.704686	0.704476	0.704395	0.704502	0.704198
$^{147}Sm/^{144}Nd$	0.14				0.15	0.14	0.15	0.14	0.15	0.16	0.15	0.17	0.15	0.13
$^{143}Nd/^{144}Nd$	0.512752				0.512730	0.512684	0.512719	0.512735	0.512758	0.512835	0.512716	0.512828	0.512745	0.512770
1σ	0.000005				0.000008	0.000008	0.000009	0.000008	0.000007	0.000007	0.000007	0.000009	0.000010	0.000008
$^{143}Nd/^{144}Nd_i$	0.512700				0.512676	0.512632	0.512665	0.512684	0.512702	0.512776	0.512660	0.512765	0.512689	0.512720
$\varepsilon_{Nd}(t)$	2.64				2.17	1.31	1.95	2.33	2.68	4.13	1.85	3.90	2.42	3.03

TABLE S4-2

TABLE S4. CONTINUE

Sample	11DZ-18	11DZ-19	11DZ-20	11DZ-21	11DZ-23	13DZ-02	13DZ-03	13DZ-04	13DZ-09	13DZ-10	13DZ-11	13DZ-15	13DZ-16
SiO_2	50.74	52.17	52.36	53.23	55.52	53.34	53.09	53.01	52.90	49.21	48.18	51.56	54.06
TiO_2	0.76	0.82	1.16	1.12	0.93	1.04	0.98	1.02	1.01	0.94	0.95	0.73	0.82
Al_2O_3	14.66	16.01	17.93	17.87	17.73	16.92	17.02	17.22	17.06	17.73	18.03	14.29	14.99
Fe_2O_{3T}	9.95	9.67	11.50	11.03	8.95	10.38	10.40	10.15	10.56	10.97	11.08	8.95	8.11
MnO	0.15	0.15	0.19	0.19	0.14	0.20	0.23	0.23	0.21	0.21	0.21	0.22	0.19
MgO	9.73	7.28	4.74	4.32	3.36	3.86	3.29	2.94	3.67	5.92	5.68	9.55	7.47
CaO	9.98	9.57	5.53	5.64	6.82	4.18	7.06	8.07	6.12	5.27	5.82	8.49	7.20
Na_2O	2.34	2.75	3.72	3.63	3.30	3.62	3.57	3.28	3.88	3.36	3.49	2.43	2.73
K_2O	0.60	0.57	1.63	1.80	1.33	3.16	1.23	1.05	1.28	2.30	2.20	1.34	1.93
P_2O_5	0.10	0.09	0.22	0.24	0.22	0.26	0.24	0.26	0.26	0.19	0.18	0.10	0.13
LOI	0.60	0.58	0.63	0.58	1.15	2.73	2.58	2.46	2.78	3.63	3.95	2.03	2.31
Total	99.60	99.65	99.62	99.64	99.44	99.68	99.70	99.69	99.72	99.73	99.78	99.70	99.95
Mg#	68.3	62.4	47.6	46.3	45.2	45.0	41.0	38.9	43.4	54.3	50.4	70.1	67.0
Sc	29.97	26.25	28.42	26.75	17.34	29.78	27.77	28.95	29.71	29.65	30.92	30.63	33.16
V	211.7	210.6	204.0	190.2	173.3	204.6	198.7	200.5	204.8	235.8	261.1	215.3	204.3
Cr	601.00	530.20	48.90	39.64	14.43	19.30	48.22	65.26	15.05	24.26	47.31	497.40	400.80
Co	41.01	31.98	30.38	27.69	20.97	25.46	24.37	23.26	26.80	34.45	32.05	41.06	36.40
Ni	178.60	121.30	5.72	5.01	9.53	10.28	6.27	7.31	7.90	13.38	11.36	168.60	101.50
Rb	10.22	10.35	33.64	34.78	33.67	96.99	21.64	17.23	23.48	79.12	61.65	56.61	75.05
Ba	165.9	124.3	577.1	555.0	376.2	1003.2	329.6	221.7	373.1	473.1	546.8	145.4	282.2
Th	1.13	1.45	1.92	1.98	2.46	2.12	2.04	2.06	2.08	1.46	1.37	3.91	5.86
U	0.35	0.50	0.62	0.61	0.68	0.62	0.60	0.62	0.64	0.38	0.37	1.53	1.79
Nb	1.64	1.96	3.43	3.57	4.21	3.81	3.66	3.72	3.82	2.83	2.74	2.28	3.49
Ta	0.15	0.14	0.24	0.25	0.31	0.23	0.23	0.23	0.23	0.16	0.16	0.25	0.34
La	6.01	6.89	12.49	13.12	15.11	13.09	12.35	13.71	13.03	9.52	9.30	7.65	12.16
Ce	13.44	15.43	28.11	29.38	32.25	29.96	28.17	31.37	29.58	22.74	22.05	16.86	27.63
Pb	3.99	5.64	6.45	6.91	9.36	16.15	13.66	11.23	11.76	5.82	8.49	5.91	5.98
Pr	1.93	2.17	3.68	3.97	3.98	4.16	3.90	4.26	4.14	3.05	2.97	2.23	3.54
Sr	395.1	484.5	364.6	390.8	483.3	447.1	537.3	616.5	453.9	387.0	394.2	288.3	317.0
Nd	8.84	9.93	16.28	17.57	16.97	18.50	17.27	18.83	18.45	13.65	13.34	9.66	15.01
Zr	57.21	68.05	97.98	98.93	44.55	105.30	99.48	100.70	104.30	68.57	66.86	67.28	105.40
Hf	1.43	1.68	2.35	2.42	1.29	2.82	2.71	2.75	2.80	2.01	1.95	2.05	2.86
Sm	2.40	2.60	4.17	4.53	3.83	4.58	4.22	4.61	4.54	3.43	3.39	2.42	3.58
Eu	0.82	0.85	1.19	1.27	1.21	1.29	1.25	1.37	1.33	1.05	1.09	0.78	1.07
Ti	4295	4517	6033	5978	5363	6049	5635	5906	5950	5398	5566	4318	4695
Gd	2.62	2.80	4.22	4.67	3.73	4.49	4.23	4.50	4.48	3.51	3.39	2.55	3.63
Tb	0.46	0.49	0.73	0.78	0.62	0.74	0.68	0.74	0.74	0.58	0.56	0.42	0.59
Dy	2.82	2.96	4.46	4.75	3.46	4.69	4.34	4.66	4.67	3.67	3.59	2.65	3.70
Y	14.53	15.10	22.93	23.30	17.59	25.03	23.43	24.92	24.87	19.88	19.41	14.42	21.07
Ho	0.63	0.64	0.98	1.05	0.76	1.00	0.92	0.99	0.99	0.79	0.77	0.56	0.79
Er	1.67	1.88	2.71	2.94	1.95	2.79	2.58	2.76	2.75	2.22	2.15	1.55	2.21
Tm	0.25	0.26	0.42	0.43	0.28	0.40	0.38	0.40	0.40	0.32	0.31	0.22	0.32
Yb	1.63	1.79	2.55	2.73	1.89	2.59	2.45	2.57	2.59	2.12	2.06	1.45	2.07
Lu	0.25	0.26	0.40	0.41	0.27	0.41	0.38	0.40	0.40	0.33	0.32	0.23	0.33
$^{87}Rb/^{86}Sr$	0.07	0.06	0.27	0.26				0.08	0.15	0.59			
$^{87}Sr/^{86}Sr$	0.704529	0.704506	0.704656	0.704675				0.704546	0.704568	0.704647			
1σ	0.000003	0.000006	0.000003	0.000004				0.000012	0.000009	0.000015			
$^{87}Sr/^{86}Sr_i$	0.704469	0.704456	0.704440	0.704466				0.704480	0.704447	0.704169			
$^{147}Sm/^{144}Nd$	0.16	0.16	0.16	0.16				0.15	0.15	0.15			
$^{143}Nd/^{144}Nd$	0.512819	0.512782	0.512819	0.512771				0.512780	0.512782	0.512805			
1σ	0.000008	0.000008	0.000010	0.000008				0.000008	0.000008	0.000008			
$^{143}Nd/^{144}Nd_i$	0.512758	0.512723	0.512761	0.512713				0.512725	0.512726	0.512748			
$\varepsilon_{Nd}(t)$	3.77	3.09	3.83	2.89				3.13	3.15	3.58			

Fe_2O_3t means iron is given as total Fe_2O_3. In the following calculation, the total FeO=0.8998×Fe_2O_3t.

TABLE S5

TABLE S5. MODELING RESULTS OF PRIMACALC2 FOR PRIMARY MAGMA COMPOSITIONS OF REPRESENTATIVE MAFIC SAMPLES FROM DAZI AREA, SOUTHERN TIBET

Element	Input	Output	Input	Output
Sample	11DZ-06	11DZ-06**P***	11DZ-19	11DZ-19**P***
SiO_2	53.95	52.86	52.17	51.33
TiO_2	0.79	0.69	0.82	0.70
Al_2O_3	15.12	13.24	16.01	13.71
FeO	7.47	7.98	8.70	9.04
MnO	0.11	0.11	0.15	0.15
MgO	7.45	13.40	7.28	13.44
CaO	9.18	8.08	9.57	8.76
Na_2O	2.59	2.26	2.75	2.32
K_2O	1.50	1.31	0.57	0.48
P_2O_5	0.09	0.08	0.09	0.08
Total	98.27	100.00	98.10	100.00
Rb	53.26	44.53	10.35	8.32
Ba	205.3	171.6	124.3	99.9
Th	4.94	4.13	1.45	1.16
U	1.58	1.32	0.50	0.40
Nb	3.16	2.64	1.96	1.58
Ta	0.32	0.27	0.14	0.11
K	12486	10440	4735	3805
La	10.47	8.77	6.89	5.58
Ce	22.70	19.01	15.43	12.52
Pb	5.59	4.68	5.64	4.54
Pr	2.92	2.45	2.17	1.76
Sr	329.50	275.67	484.50	393.89
Nd	12.69	10.62	9.93	8.12
Sm	3.06	2.56	2.60	2.14
Zr	96.22	80.61	68.05	55.33
Hf	2.37	1.99	1.68	1.38
Eu	0.93	0.78	0.85	0.70
Gd	3.06	2.56	2.80	2.31
Tb	0.56	0.47	0.49	0.41
Dy	3.38	2.84	2.96	2.46
Y	17.31	14.52	15.10	12.55
Ho	0.73	0.61	0.64	0.53
Er	2.04	1.71	1.88	1.56
Tm	0.30	0.25	0.26	0.22
Yb	1.96	1.65	1.79	1.48
Lu	0.29	0.24	0.26	0.22
Ni	97.50	352.06	121.30	411.21
Ni(ol)wt%		0.36		0.40
Fo(ol)%		91.7		90.6
Mg# Bas		75		73
$Fe^{2+}/Fe(t)$		0.83		0.83
H_2O(wt %)		0.99		0.99
T (□)		1355		1368
P (GPa)		1.0		1.0
F%(Herz)		5		5
%Xfrac.		18		21
MgO PM		45		39

Abbreviations: **P***: the primitive melt. **Ni(ol)wt%**: Ni concentration in olivine equilibrated with the mantle. **Fo(ol)%**: forsterite content in olivine equilibrated with the mantle. **Mg# bas**: Mg# of primary magma. **$Fe^{2+}/Fe_{(t)}$**: ferric/total iron ratio in primary magma. **H_2O (wt %)**: water contents in primary magma. **T (°C)**: temperature (**°C**) of hydrous primary magma according to the method of Katz et al. (2003). **P (GPa)**: the pressure of melting depth for producing the primary magma calculated by peridotite equilibrium. **F%(Herz)**: degree of partial melting in the source mantle estimated by Herzberg et al. (2007). **%Xfrac.**: crystal fractionation calculated by PRIMACLC2. **MgO PM**: MgO wt% in the source mantle. **Input**: target magma composition; **Output**: modeled primary magma composition.

TABLE S6

TABLE S6. FORWARD MODELING RESULTS OF ABS5

Sample and Model results	11DZ-06P*	Mean ABS5 Results[1]	1σ	Mean ABS5 Results[2]	1σ	11DZ-19P*	Mean ABS5 Results[1]	1σ	Mean ABS5 Results[2]	1σ
Melting condition										
Slab P(GPa)		3.9	0.3	4.1	0.2		4.0	0.4	4.0	0.2
Slab T(℃)		865	8	931	8		869	11	927	9
%R slab		145	19	157	22		152	22	141	28
Fliq(AOC)		0.52	0.07	0.38	0.06		0.52	0.11	0.51	0.07
Fliq(SED)		0.31	0.09	0.42	0.11		0.27	0.12	0.19	0.08
Fliq(DMM)		0.18	0.08	0.20	0.11		0.21	0.08	0.30	0.08
n(PERID)		0	0	0	0		0	0	0	0
Pperid (GPa)		1.5	0.2	1.2	0.1		1.3	0.2	1.1	0.1
Tperid (C)		1186	44	1220	49		1216	40	1253	25
%MORBext.		0	0	0	0		0	0	0	0
Fslb liq.%		5.4	0.8	3.2	0.8		3.9	0.6	1.7	0.4
H2O% in SLBliq		19.2	7.2	20.9	11.3		22.2	8.0	30.4	7.7
H2O% in PERID		1.0	0.4	0.7	0.5		0.9	0.4	0.5	0.2
F(%)PERID		15	1	17	2		19	1	20	1
β (%)		28	4	15	3		16	3	7	1
Major and trace elements										
SiO2	52.86	48.08	0.80	48.28	0.82	51.33	48.21	0.84	48.02	0.69
TiO2	0.69	0.60	0.02	0.57	0.02	0.70	0.55	0.02	0.52	0.02
Al2O3	13.24	13.76	0.55	13.87	0.54	13.71	13.58	0.57	13.26	0.37
FeO	8.87	11.36	0.72	9.93	0.74	10.04	10.56	0.77	9.44	0.48
MgO	13.40	14.04	0.73	13.66	0.80	13.44	14.14	0.83	14.30	0.66
CaO	8.08	9.12	0.30	10.49	0.33	8.76	10.27	0.33	11.11	0.37
Na2O	2.26	2.26	0.00	2.26	0.00	2.32	2.32	0.00	2.32	0.00
K2O	1.31	0.75	0.20	0.92	0.35	0.48	0.36	0.16	1.02	0.38
H2O		6.7	2.3	4.0	2.4		4.7	1.8	4.0	1.8
Rb	44.53	5.50	1.75	14.24	11.38	8.32	2.91	0.80	16.37	9.87
Ba	171.6	377	73	297	47	99.9	198.6	56.6	195.9	51
Th	4.13	1.76	0.25	1.84	0.14	1.16	1.10	0.27	0.72	0.18
U	1.32	0.61	0.05	0.65	0.06	0.40	0.40	0.05	0.32	0.06
Nb	2.64	2.95	0.15	3.25	0.37	1.58	2.10	0.12	1.99	0
Ta	0.27	0.17	0.01	0.21	0.02	0.11	0.12	0.01	0.11	0.01
K	10440	6258	1664	7654	2898	3805	2965	1324	8426	3127
La	8.77	8.93	0.51	7.82	0.71	5.58	5.72	0.42	4.86	0.60
Ce	19.01	26.37	1.60	22.27	2.33	12.52	16.91	1.20	14.47	1.78
Pb	4.68	7.27	1.09	6.67	0.43	4.54	4.20	1.05	3.57	1
Pr	2.45	2.35	0.12	2.25	0.22	1.76	1.68	0.10	1.40	0.15
Sr	276	371	31	287	33	394	218	33	212	40
Nd	10.62	8.70	0.43	8.51	0.80	8.12	6.53	0.34	5.67	0.6
Sm	2.56	1.82	0.11	1.84	0.13	2.14	1.51	0.06	1.44	0.10
Zr	80.6	43.17	1.84	46.47	3.32	55.3	35.6	1.4	34.0	3.13
Hf	1.99	1.41	0.05	1.50	0.11	1.38	1.16	0.04	1.10	0.07
Eu	0.78	0.61	0.04	0.61	0.05	0.70	0.53	0.02	0.52	0.03
Gd	2.56	2.09	0.15	2.12	0.17	2.31	1.85	0.08	1.85	0.09
Tb	0.47	0.38	0.03	0.38	0.03	0.41	0.34	0.02	0.35	0.02
Dy	2.84	2.59	0.20	2.66	0.22	2.46	2.40	0.11	2.44	0.10
Y	14.52	16.16	1.27	16.53	1.42	12.55	14.97	0.72	15.29	0.69
Ho	0.61	0.58	0.04	0.59	0.05	0.53	0.54	0.03	0.55	0.02
Er	1.71	1.71	0.13	1.76	0.15	1.56	1.60	0.07	1.65	0.06
Tm	0.25	0.26	0.02	0.27	0.02	0.22	0.24	0.01	0.25	0.01
Yb	1.65	1.63	0.11	1.70	0.12	1.48	1.57	0.07	1.64	0.06
Lu	0.24	0.26	0.02	0.27	0.02	0.22	0.25	0.01	0.26	0.01
Residual mantle mode										
Ol		0.57	0.02	0.64	0.02		0.63	0.02	0.69	0.01
Opx		0.33	0.02	0.30	0.02		0.32	0.02	0.28	0.01
Cpx		0.07	0.01	0.04	0.01		0.03	0.01	0.00	0.00
Gar		0	0	0	0		0	0	0	0.00
Sp		0.03	0.00	0.03	0.00		0.03	0.00	0.02	0.00

Note: **superscript [1]**: slab geotherm from North Chile subduction zone for ABS5 modelling. **superscript [2]**: slab geotherm from Colombia-Ecuador subduction zone for ABS5 modelling.

Abbreviations: **P***: the primitive melt calculated by PRIMACALC2 (Kimura and Ariskin 2014). **ABS5**: Arc Basalt Simulator version 5; **Slab P(GPa)**: depth of slab melt release; **Slab T (°C)**: slab surface temperature at slab melt release; **R% slab**: the reactivity degree between the liquids and solids; **Fliq(AOC)**: slab flux contribution from altered oceanic crust; **Fliq(SED)**: slab flux contribution from sediment. **Fliq(MwP)**: slab flux contribution from metasomatized mantle wedge peridotite. **n(PERID)**: zone refining reaction factor; **P_{perid} (GPa)**: partial melting depth of the source mantle; **T_{perid} (°C)**: temperature of partially molten mantle; **%MORBext.**: peridotite predepletion factor expressed by wt. % MORB melt extracted; **Fslb liq.%**: fraction of fluxed slab melt; **H2O% in SLBliq**: water content in slab melt; **H2O% in PERID**: water content in the mantle wedge peridotite; **F(%)PERID**: degree of partial melting of peridotite; **β (%)**: beta factor of flux melt fraction = [β/(α+β)]×100. **Ol**: olivine; **Opx**: orthopyroxene; **Cpx**: clinopyroxene; **Gar**: garnet; **Sp**: spinel. Iron is given as total FeO.